A novel MARV glycoprotein-specific antibody with potentials of broad-spectrum neutralization to filovirus

Running title: An anti-filovirus antibody fused with NPC2

Yuting Zhang[1,2†], Min Zhang[1†], Haiyan Wu[1†], Xinwei Wang[1,2†], Hang Zheng[1,2], Junjuan Feng[1,2], Jing Wang[1], Longlong Luo[1], He Xiao[1], Chunxia Qiao[1], Xinying Li[1], Yuanqiang Zheng[2], Weijin Huang[3], Youchun Wang[3], Yi Wang[4*], Yanchun Shi[2*], Jiannan Feng[1*], Guojiang Chen[1*]

[1]State Key Laboratory of Toxicology and Medical Countermeasures, Institute of Pharmacology and Toxicology, Beijing, China

[2]Inner Mongolia Key Lab of Molecular Biology, School of Basic Medical Sciences, Inner Mongolia Medical University, Hohhot, China

[3]Division of HIV/AIDS and Sex-transmitted Virus Vaccines, National Institutes for Food and Drug Control, Beijing, China

[4]Department of Hematology, Fifth Medical Center of Chinese PLA General Hospital, Beijing, China

*Address correspondence to Yi Wang, yk091023@163.com; Yanchun Shi, ycshi5388@163.com; Jiannan Feng, fengjiannan1970@qq.com or Guojiang Chen, jyk62033@163.com.

†These authors contributed equally to this work

Abstract

Marburg virus (MARV) is one of the filovirus species that causes a deadly hemorrhagic fever in humans, with mortality rates up to 90%. Neutralizing antibodies represent ideal candidates to prevent or treat virus disease. However, no antibody has been approved for MARV treatment to date. In this study, we identified a novel human antibody named AF-03 that targeted MARV glycoprotein (GP). AF-03 possessed a high binding affinity to MARV GP and showed neutralizing and protective activities against the pseudotyped MARV in vitro and in vivo. Epitope identification, including molecular docking and experiment-based analysis of mutated species, revealed that AF-03 recognized the Niemann-Pick C1 (NPC1) binding domain within GP1. Interestingly, we found the neutralizing activity of AF-03 to pseudotyped Ebola viruses (EBOV, SUDV, and BDBV) harboring cleaved GP instead of full-length GP. Furthermore, NPC2-fused AF-03 exhibited neutralizing activity to several filovirus species and EBOV mutants via binding to CI-MPR. In conclusion, this work demonstrates that AF-03 represents a promising therapeutic cargo for filovirus-caused disease.

Keywords Marburg, glycoprotein, neutralizing antibody, NPC1, filovirus, NPC2

Introduction

Filoviruses are a nonsegmented negative-sense RNA viruses, comprised of six genera, Ebolavirus, Marburgvirus, Cuevavirus, Striavirus, Thamnovirus and a recently discovered sixth genus, Dianlovirus[1-3]. The Marburgvirus genus consists of Marburg virus (MARV) and Ravn virus (RAVN)[1,4,5]. The former includes three strains-- Uganda, Angola and Musoke. The Ebola virus genus includes six distinct species Zaire Ebola virus (EBOV), Bundibugyo virus (BDBV), Sudan virus (SUDV), Reston virus (RESTV), Taii Forest virus (TAFV) and Bombali virus (BOMV), the first three of which cause severe hemorrhagic fevers[6,7]. The genus Cuevavirus (Lloviu virus, LLOV) was isolated from Miniopterus schreibersii bats in Spain and Hungary and potently infected monkey and human cells[8,9]. The genus Měnglà virus (MLAV) was discovered in the liver of a bat from Mengla, Yunnan, China in 2019. So far, only an almost complete RNA sequence of the viral genome is available, there are no viable MLAVs isolated.[10] MARV and EBOV infect humans and non-human primates, causing Marburg virus disease (MVD) and EBOV virus disease (EVD) with an incubation period of 2-21 days[11]. The symptoms of MVD include severe headache and high fever rapidly within 5 days of the onset of symptoms, followed by diarrhea and vomiting, leading to up to 90% fatality rate[11]. MARV and EBOV have a high potential to cause a public health emergency.

Glycoprotein (GP) on the surface of filoviruses is a type I transmembrane protein and consists of GP1 and GP2 subunits[12,13]. It is inserted into the virus envelope in the form of homotrimeric spikes[14] and is responsible for virus attachment and entry. The

furin cleaves Marburg GP at the amino acid 435 into two subunits, GP1 and GP2, which remains linked by a disulfide bond[15]. GP1 contains a receptor binding domain (RBD), a glycan cap, and a heavily glycosylated mucin-like domain (MLD), which mediates binding to entry factors and receptors[16]. GP2 has a partial MLD, a transmembrane domain for viral anchoring to the envelop surface, and a fusion peptide required for the fusion of virus and cell membranes[17-19]. In the Ebola virus, the furin cleavage site is located at residue 501 and the entire MLD is attached to the GP1 subunit[20]. Marburg virus contains 66 amino acids on GP2 that are absent from the Ebola virus MLD, and are called "wings" due to their outward projection and flexibility[17].

Currently, GP is a major target for antibodies validated in filovirus-infected animals and clinical trials because it is exposed on the surface of the virus and plays a key role in viral entry[21]. Filoviruses initially enter cells by endocytosis[22,23]. Once inside the endosome, GP is cleaved by host cathepsins and glycan cap and MLD are removed, enabling GP to bind to the Niemann-Pick C1 (NPC1) receptor[24,25]. Interestingly, Ebola virus entry requires cathepsin B cleavage[26], which is redundant for Marburg virus entry[27,28]. Hashiguchi et al. propose that the receptor binding domain is masked by glycan cap and MLD in the Ebola virus, whereas it is partially exposed in the Marburg virus[16].

To date, there is no licensed treatment or vaccine for Marburg infection. Herein, we utilized phage display technology to screen an antibody in a well-established antibody library[29,30] and obtained a novel human antibody with prominent neutralizing

activity. Furthermore, NPC2 fusion at the N terminus of the light chain of this antibody renders broad-spectrum inhibition of cell entry of filovirus species and mutants.

Materials and methods

Cell lines and plasmids

Human embryonic kidney cells HEK293T and human hepatoma cells Huh7 were purchased from ATCC. These cell lines were cultured in Dulbecco's modified Eagle's medium (DMEM) (Gibco, 11965e092) supplemented with 100 units/ml penicillin, 100 units/ml streptomycin (Gibco, 15140) and 10% fetal bovine serum (Gibco, 10099) in a humidified atmosphere (5% CO_2, 95% air) at 37°C. ExpiCHO-S cells were purchased from Gibco and cultured in ExpiCHO™ Expression Medium (Gibco, A29100) in a humidified atmosphere (8% CO_2, 92% air) on an orbital shaker platform.

MARV (AFV31370.1), Angola (Q1PD50.1), Musoke (YP_001531156.1), Ravn (YP_009055225.1), TAFV (Q66810), RESTV (Q66799), BOMV (YP_009513277.1) MLAV (YP_010087186.1), LLOV (JF828358) GPs plasmid synthesized by GENEWIZ and then cloned into the expression vector pcDNA3.1. EBOV (A0A068J419), BDBV (AYI50382), SUDV (Q7T9D9) GPs and HIV-based vector pSG3. Δenv. cmvFluc plasmids were kindly gifted by China Institute for Food and Drug control.

Preparation of full-length antibody and antigen

AF-03 was selected from a human phage antibody library, which displays on the surface of M13 bacteriophage particles. Screening procedures were as described in detail previously[34,35]. Phage antibodies that bound to MARV GP protein were obtained to express full-length IgGs using a standard protocol. In brief, the VH and

VL region of AF-03 were constructed into a mammalian full-length immunoglobulin expression vector pFRT-KIgG1 (Thermo, V601020), to generate plasmid AF-03. The human NPC2 gene (aa20-151) was linked to the VL of AF-03 by a short linker "TVAAP" and then constructed into pFRT-KIgG1 (designated as AF03-NL). The AF-03 and AF03-NL plasimid were transfected into ExpiCHO-S cells using the ExpiFectamine™ CHO Transfection Kit (Gibco, A29129) following the manufacturer's instructions. Purification was performed using ÄKTA prime plus system (GE Healthcare) with protein A column (GE Healthcare). MARV GP (Uganda strain) (aa 20-648, Δ277-455), CI-MPR1-3 (aa36-466) and NPC2 (aa20-151) gene with six-histidine-tagged at C-terminus was cloned into mammalian expression vector pcDNA3.1 and then transfected into HEK293T cells. MARV GP was purified using nickel column (GE Healthcare, 11003399). The concentration of proteins and antibodies were quantified by bicinchoninic acid (BCA) method.

ELISA

The 96-well enzyme-labelled array plates were coated with 2 μg/ml MARV-GP and mutated MARV GP ($Q^{128}S$-$N^{129}S$) respectively and incubated overnight at 4°C. Wells were washed for three times and blocked for 1 h at 37°C. A series of 12 concentrations of AF-03 and MR78 were added and incubated for 1 h at 37 °C. Bound antibodies were detected with horseradish peroxidase (HRP)-labeled goat anti-human IgG secondary antibody (Invitrogen, A18817) at room temperature for 30 min. Binding signals were visualized using a TMB substrate (CWBIO, CW0050S) and the reaction was stopped by adding 2 N H_2SO_4. The light absorbance at 450 nm was

measured by microplate reader (Thermo Fisher Scientific). The concentration for 50% of maximal effect was defined as EC_{50}.

For competitive ELISA, biotinylated AF-03 (1 μg/ml) was coated. MR78 and control mAb (Herceptin) in 3-fold serial dilution (ranging from 0.27 to 200 ug/ml) and added to the plates. After 1 h incubation at 37°C, the plates were washed and the bound Biotin-AF-03 was detected by adding horseradish peroxidase (HRP)-labeled Streptavidin (Thermo, S911). After a further 30 min incubation at room temperature, the plates were washed and TMB was added. The reaction was stopped by adding 2 N H_2SO_4. Absorbance was measured at 450 nm using a plate reader.

BLI analysis of antibody affinity

The binding affinity of AF-03 to MARV GP was measured by the Fortebio biofilm interferometry technique using anti-huamn IgG Fc capture (AHC) biosensors. In brief, 8 μg/ml antibody was diluted to PBS containing 0.02% Tween 20 and immobilized in biosensors. The biosensors were then immersed with a serial dilutions of MARV GP to determine the association constant. Programs setting were following: baseline 60 s, loading 60 s, baseline 60 s, association 180 s, dissociation 220 s, regeneration 5 s. Baseline was performed with PBST buffer and regeneration was performed with 10 mM glycine-HCl (pH 1.7) thrice. The data were analyzed using FortéBio Data Analysis 9.0 (Sartorius, FortéBio®).

Computer□guided homology modeling and molecular docking

The three-dimensional theoretical structure of fragment variable (FV) was constructed using computer-guided homology modeling approach based on the amino acid

sequences of the variable structural domains of the heavy and light chains of AF-03, and the conserved regions and loop structural domains were identified. The 3-D structure of the AF-03 Fv fragment was optimized under the consistent valence force field (CVFF) using the steepest descent and conjugate gradient minimization methods. The final minimized 3-D structure was evaluated by means of Ramachandran diagrams. In addition, the 3-D theoretical structure of the MARV GP protein was obtained and optimised using the CVFF force field. Under molecular docking method, the 3-D complex structures AF-03 Fv fragment and GP were obtained and optimized. With the determined 3-D structure of the AF-03 Fv fragment and GP, 50-ns molecular dynamics were performed with the Discovery_3 module. All calculations were performed using Insight II 2000 software (MSI Co., San Diego) with IBM workstation.

Pseudovirus preparation

HIVΔenvor (pSG3.Δenv.cmvFluc) bearing MARV, mutated MARV ($Q^{128}S$-$N^{129}S$, $T^{204}A$-$Q^{205}A$-$T^{206}A$, $Y^{218}A$, $K^{222}A$ and $C^{226}Y$), EBOV (parental and 17 mutants indicated), SUDV, BDBV, TAFV, RESTV, BOMV, RAVN, MLAV and LLOV GPs were prepared by liposome-mediated transfection of HEK293T cells using JetPRIME (Polyplus Transfection, 25Y1801N5). Cells were seeded in 6-well plates at a density of 7×10^5cells/well and transfected with 2 μg plasmids (0.4 μg GP and 1.6 μg HIVΔenvor) when cells reached 60-80% confluence. Supernatants were collected 48 h after transfection, centrifuged to remove cell debris at 3,000 rpm for 10 min, filtered through a 0.45 μm-pore filter (Millipore,SLHUR33RB) and stored at -80°C.

Pseudovirus entry and antibody neutralization assay

Huh7 and HEK293T cells ($3x10^4$ cells/100 μl/well) were infected with 100 μl pseudovirus, which contained a luciferase reporter gene respectively. The luciferase activity were measured in a fluorescence microplate reader (Promega). The operation steps were following: after 36 h incubation at 37°C, 100 μl of culture medium were discarded and addition with 100 μl of Bright-Glo luciferase reagent (Promega, E6120) in each well. Mixtures were transfered to 96-well whiteboards after 2-minutes reaction to detect the relative luciferase intensity.

For AF-03 neutralization of MARV assays, 50 μl mAb was 3-fold serially diluted and separately mixed with MARV pseudovirus at the same volume. The mixture were incubated at 37°C for 1 h, followed by the addition of 100 μl cells ($3x10^4$ cells/well). 50% of maximal inhibitory concentration was defined as IC_{50}. IC_{50} values were determined by non-linear regression with least-squares fit in GraphPad Prism 8 (GraphPad Software).

In terms of AF-03 neutralization of ebola virus assays, pseudovirus (EBOV, SUDV and BDBV) were processed with thermolysin as previously described [36]. Briefly, Pseudotyped ebola virus were incubated at 37°C for 1 h with 200 μg/ml thermolysin (Sigma, T7902). The reaction was stopped by addition of 400 μM Phosphoramidon (Sigma, R7385) on ice for 20 min. The remaining steps followed AF-03 neutralization of MARV assays.

For AF03-NL neutralization assays, 50 μl/well of serial diluted AF03-NL and AF-03 were incubated with cells at 37°C for 2 h to enable internalization of the

antibodies. 50 μl/well of diluted pseudovirus was added to a 96-well plate and incubated at 37°C for 36 h. Bright-Glo luciferase reagent was added to detect the relative luciferase intensity.

Bioluminescent imaging in vivo

Four-week-old female BALB/c mice were purchased from Beijing Vital River Laboratory Animal Technology Co. Ltd. Mice were intraperitoneally injected with MARV pseudovirus (0.2 ml/mouse). AF-03 (10, 3 or 1 mg/kg) or control antibody Herceptin (10 mg/kg) were injected via intravenous route 24 h and 4 h before the pseudovirus injection respectively. Bioluminescent signals were monitored at Day 5. Briefly, D-luciferin (150 mg/kg body weight) (PerkinElmer, 122799) was intraperitoneally injected into the mice, and then exposed to Isoflurane alkyl for anesthesia. Bioluminescence was measured by the IVIS Lumina Series III Imaging System (Xenogen, Baltimore, MD, USA) with the living Image software. The signals emitted from different regions of the body were measured and presented as total fluxes. All data are presented as mean values ± SEM.

Evaluation of internalization

HEK293T cells were counted 3×10^5 cells, cold PBS washed twice and discarded the supernatant. 20 μg/ml AF-03/AF03-NL was added and incubated at 4°C for 30 min. Then internalization group was transferred to 37°C for internalization for 30 min, while the control group continued to be incubated at 4°C for 30 min to adhere to the cell surface. The cells were washed with cold PBS, PE-anti-human IgG Fc secondary antibody (Biolegend, 41070) was added and incubated for 30 min at 4°C. The cells

were collected for analysis.

pHrodo Red labelling and immuno-localization

AF03-NL and AF-03 were covalently labeled with pH-sensitive pHrodo red succinimidyl ester (Thermo, P36600) according to the manufacturer's instructions. Antibodies were incubated with 10-fold molar excess of pHrodo red succinimidyl ester for 1 h at room temperature. Excess unconjugated dye was removed using PD-10 desalting columns (GE Healthcare). pHrodo Red-labeled antibodies were exchanged into HEPES buffer and concentrated in an Amicon Ultra centrifugal filter unit with a nominal molecular weight cutoff of 30 kDa. Antibody concentration and degree of labeling was determined according to the manufacturer's instructions.

HEK293T cells ($1\sim2\times10^5$ cells per dish) were cultured overnight in confocal dish pre-treated with polylysine (Beyotime, ST508) and then incubated with pHrodo Red-labeled AF-03 and AF03-NL (20 μg/ml) at 37°C for 30 min. Unbound antibodies were removed by washing with cold PBS. As well, cells were stained with cell membrane dye (DiD) (Thermo, V22887) and Hoechst33342 (Thermo, H1398) at 37°C for 15 min. Single cells were analyzed for pHrodo Red fluorescence on.Confocal Microscopy (dragonfly 200).

CI-MPR knockin and knockdown

Huh7 Cells were seeded in 6-well plates at 3×10^5 cells/well and transfected with 2 μg CI-MPR expression plasmids (JetPRIME) when cells reached 40-60% confluence and cultured for 24 h. For CI-MPR silencing, HEK293T cells were seeded in 6-well plates and transfected with siRNA-CI-MPR (Ribbio) and cultured for 48-72 h. CI-MPR

expression was detected by flow cytometry.

Flow cytometry

The cells were harvested and stained with FITC-conjugated anti-CI-MPR antibody (Biolegend, 364207) on ice for 30 min. Cells were washed twice and detected on FACSAria II (BD Biosciences). Data analysis was performed using the FlowJo software.

Statistical analyses

Data were analyzed, and the graphs were plotted using Prism software (GraphPad Prism 8, San Diego, USA). The data are presented as the mean ± standard error of the mean. Intergroup differences were compared using unpaired t-tests or ANOVA. The $P < 0.05$ was considered statistically significant.

Results

Characteristics of AF-03

AF-03 was selected from a well-established phage surface display antibodies library with immense diversity in the selected complementarity determining region (CDR) loops[34,35]. We further subcloned VH and VL sequences of the antibody into a mammalian full-length immunoglobulin expression vector for full - length IgG expression. As shown in Fig. 1A, AF-03 was eukaryotically expressed with the purity over 95%. To determine the binding affinity, recombinant MARV GP without MLD was prepared (Fig. 1A). ELISA analysis showed that AF-03 bound to MARV GP with EC_{50} of 0.16 μg/ml (Fig. 1B). Furthermore, BLI assay was done to determine the binding kinetics and showed that AF-03 bound to MARV GP with high affinity (K_D value was less than $1x10^{-12}$M) (Fig. 1C). To identify determinants of MARV GP binding to AF-03, we utilized computer-guided homology modeling and molecular docking to generate computer models of MARV GP in complex with AF-03. Firstly, we obtained the theoretical 3-D structure of AF-03 Fv (Fig. 1D). Based on the 3-D structure of AF-03 and MARV GP separately, the 3-D complex structure of AF-03 and MARV GP achieved utilizing the molecular docking method, as shown in Fig. 1E. Overall, these data suggest the potency of AF-03 binding to MARV GP.

Epitope mapping of MARV GP bound to AF-03

Under CVFF forcefield, chosen steepest descent and conjugate gradient minimization methods, after 30,000 steps of minimization with the convergence criterion 0.02 kCal/mol, the optimized structure of the AF-03 Fv was evaluated. Using

a Ramachandran plot, the assignment of the whole heavy atoms of the AF-03 Fv was in the credible range. Through analyzing the van der Waals interactions, inter-molecular hydrogen bonds, polar interactions and electrostatic interactions between AF-03 and MARV GP, the key amino acid residues of MARV GP were selected for amino acid point mutations (Fig. 1F). T^{204}-Q^{205}-T^{206}, Y^{218} and K^{222} were mutated to alanine, and Q^{128}-N^{129} were mutated to serine as well as C^{226} was mutated to tyrosine. Firstly, We investigated if this mutated MARV species was still sensitive to AF-03 treatment. The inhibition assay revealed the impairment of neutralizing activity of AF-03 to mutated MARV pseudovirus, which indicates that Q^{128}/N^{129}/C^{226} functions as key amino acids responsible for AF-03 neutralization (Fig. 2A left panel). To this end, we constructed the mutated MARV GP. ELISA assay showed that mutation of Q^{128}S-N^{129}S or C^{226}Y significantly disrupted binding of GP to AF-03, while the binding and neutralizing capacity of MR78 to mutant GP and pseudovirus (C^{226}Y), a mAb reported to be isolated from Marburg virus survivors[16], was not almost affected (Fig. 2A right panel and B). Furthermore, we analyzed the secondary structure of the MARV GP and its mutants. By circular dichroism, the structure of both mutants was not obviously different from that of the parent GP (Fig. 3C, Tab. s1). Therefore, the weakened binding to the antibody was not due to the conformational change of the protein caused by the mutation. Competitive ELISA showed that AF-03 and MR78 could compete with each other to bind to MARV GP (Fig. 3D). These results indicate the epitopes of these two mAbs overlapped partially.

In vitro neutralizing activity of AF-03

Given the high binding affinity of AF-03 to MARV GP, we sought to determine whether AF-03 could impede MARV pseudotyped viral entry. An in vitro neutralization assay was developed based on full-length MARV GP-pseudotyped virus using a HIVΔenvor (pSG3.Δenv.cmvFluc). Liver and adrenal glands have been reported to be the early targets of MARV infection [14,37]. Therefore, we first tested the entry of MARV to hepatocyte cell line (Huh7) and HEK293T cells (renal cell line) by measuring the relative luciferase intensity. These two cell lines were susceptible to MARV cell entry. We used MR78 and cetuximab as positive and negative controls respectively. As expected, cetuximab had no effects on pseutotyped MARV entry. In contrast, AF-03 actively inhibited viral entry to HEK293T cells, with IC_{50} value of 0.13 μg/ml. As well, IC_{50} of MR78 was 0.44 μg/ml (Fig. 3A left panel). In Huh7 cells, IC_{50} of AF-03 and MR78 was 0.4 and 1.03 μg/ml, respectively (Fig. 3A right panel). These results suggest that AF-03 had more potency of neutralization than MR78. We also conducted AF-03 neutralization experiments on pseudotyped Angola, Musoke and Ravn strains and showed strong and comparable neutralizing ability to all these strains (IC_{50} was 0.32, 0.12 and 0.15 μg/ml respectively) (Fig. 3B). Taken together, these data suggest that AF-03 harbors prominent neutralizing activity to MARV infection.

In vivo preventive efficacy of AF-03

To verify the in vivo preventive efficacy, AF-03 was intravenously injected into mice before pseudotyped MARV exposure (-24 h and -4 h) respectively. The bioluminescence intensity was measured on day 5 after pseudovirus injection. As

shown in Fig. 3C and D, AF-03-treated group displayed lower bioluminescence activity compared with the control group, while the treatment with control antibodies had no effects. Administration of 1 mg/kg AF-03 prior to the injection of MARV could decrease viral infection to approximately 50% level and increasing doses of AF-03 led to higher preventive efficacy. This indicates clearly that AF-03 is capable of preventing against MARV infection in a dose-dependent manner and represents a potential candidate for MARV prophylaxis.

AF-03 impedes cell entry of EBOV, SUDV and BDBV harboring GPcl

Given the close structural similarity of Marburg virus to ebola virus, to determine whether AF-03 was also available to the treatment of EBOV infection, we conducted neutralization of pseudotyped EBOV, SUDV and BDBV with AF-03. In addition, considering that glycan cap or mucin-like domain are known to mask the putative receptor-binding domain on EBOV, SUDV and BDBV GP, leading to blockade of engagement between AF-03 and GP[16]. Furthermore, in vitro cleavage of particles with thermolysin functionally mimics the cleavage due to the combination of cathepsin L and cathepsin B. Accordingly, glycan cap and mucin-like domain were enzymatically cleaved by digesting GP with 250 μg/ml thermolysin at 37°C. Consequently, the inhibitory function of AF-03 on cell entry of all three species of ebola virus bearing cleaved GP was much stronger than those bearing uncleaved GP (Fig. 4). Overall, these data suggest that AF-03 has therapeutic potentials for EBOV, SUDV and BDBV infection.

The potency of NPC2-fused AF-03 to be delivered into the endosome

Given the inability of AF-03 to transport into endosomal compartment where intact GP is cleaved by cathepsin B/L, we engaged NPC2 to the N-terminus of light chain of AF-03 (Fig. s1A), according to a protocol described previously[38]. As well, we produced the 1-3 domain of CI-MPR (Fig. s1A), which is a ligand for NPC2 and expressed on the cellular and endosomal membrane[32]. The results showed that NPC2-fused AF-03 (termed AF03-NL), rather than AF-03, bound to CI-MPR1-3 (Fig. s1B). Next we investigated the internalization of AF03-NL. AF03-NL or AF-03 was incubated with HEK293T cells, which expressed CI-MPR (Fig. s2A), at 4□ for attachment. As expected, AF03-NL instead of AF-03 adhered to the cell surface, detected by fluorescence-labelled secondary IgG. Upon endocytosis, the fluorescence on the cell surface decreased dramatically, implying the occurrence of AF03-NL internalization (Fig. 5A). To further address this issue, AF-03 and AF03-NL were labelled by pHrodo Red dye that is sensitive to acidic niche. Accord with Fig. 5A, pHrodo Red-conjugated AF03-NL was observed in the acidic endosomal compartment by flow cytometry and fluorescence microscopy respectively (Fig. 5B and C). In contrast, AF-03 was not seen in the endosome.

Pan-filovirus inhibition of cell entry by AF03-NL via engagement between NPC2 and CI-MPR

We first compared the binding of AF03-NL/AF-03 to MARV GP. ELISA showed relatively weak binding activity of AF03-NL compared with AF-03 (Fig. s3A). We thereafter evaluated the neutralizing activity of AF03-NL to MARV pseudovirus. Intriguingly, AF03-NL showed stronger neutralizing activity than AF-03 (The IC_{50}

was 0.057 and 0.284 μg/ml, respectively) (Fig. s3B), which may be attributed to sustained tethering of AF03-NL to pseudovirus at extracellular space as well as endosomal compartment. Next we compared the neutralizing activity of AF03-NL and AF-03 to a series of filovirus species. AF03-NL displayed superior neutralizing activity to other nine filovirus species. While, no or weak inhibition of entry by AF-03 was found (Fig. 6A). Furthermore, AF03-NL, instead of AF-03, also actively inhibited cell entry of 17 EBOV mutants that were detected in natural hosts (Fig. 6B).

To investigate the mechanisms mediating the potency of AF03-NL, we produced NPC2 protein (Fig.7A) and then examined the inhibition of EBOV entry by AF03-NL or the mixture of AF-03 and NPC2. AF-03, NPC2 alone or in combination did not inhibit EBOV entry. Conversely, AF03-NL actively impeded this process (Fig. 7B). To clarify whether this effect is CI-MPR-dependent, CI-MPR in HEK293T cells was silenced (Fig. 7C). The result showed that CI-MPR knockdown rendered significant abrogation of the inhibitory ability of AF03-NL (Fig. 7C). We also introduced CI-MPR into Huh7 cell line that is null for this receptor (Fig. s2B). The inhibitory effects of AF03-NL were augmented in CI-MPR-overexpressed cells compared with empty vector-introduced counterparts (Fig. 7D). Taken together, these data indicate that the inhibitory potency of AF03-NL is dependent on the interaction between NPC2 and CI-MPR.

Discussion

The Marburg virus was initially identified after simultaneous outbreaks in Marburg and Frankfurt in Germany in 1967[16,39]. To date, there have been a dozen outbreaks of Marburg virus infection in humans[40]. Giving the recurrence of Marburg virus outbreaks and its high virulence and lethality, there is an urgent need to develop prophylactic and therapeutic interventions for Marburg infections. MARV GP is a surface viral protein, which is responsible for host receptor binding and cell entry thus provides an attractive target for the development of antagonists. Flyak et al. screened several MARV GP-specific neutralizing antibodies from the plasma of a MARV-infected survivor, which achieved 100% protection in mice subjected to mouse-adapted MARV challenge[41]. The MARV GP-specific antibody cocktail was also developed, 3 mAbs cocktail could protect hamster from lethal hamster-adapted MARV infection, while treatment with either one or two antibodies failed[42].

In this study, we selected an antibody from a human antibody phage library and the affinity constant reached the $1x10^{-12}$M level. The neutralizing activities of the antibody were demonstrated by utilizing pseudotyped MARV Uganda strain. The results showed that AF-03 effectively inhibits HIVΔenvor (pSG3.Δenv.cmvFluc) pseudotyped MARV viral entry at IC_{50} of 0.13 and 0.4 μg/ml in HEK293T and Huh7 respectively. Furthermore, compared with control antibody, AF-03 exhibited a protective property against pseudovirus infection in mice. Epitope mapping results showed that GP Q^{128}-N^{129} and C^{226} was the binding and functional epitope that interacted with AF-03, which means AF-03 targeting the interface of GP-NPC1

interaction, considering that N129 is known to be located in the NPC1 binding domain. RBDs are highly conserved among filovirus species, so they are an attractive target for broadly effective anti-filovirus drug development[49]. We found that AF-03 also bound to EBOV GPcl and can neutralized ebola viruses bearing in vitro cleaved GP, suggesting that AF-03 represents a good candidate for endosome-delivering strategy by ligation to another mAb against a surface-exposed EBOV GP epitope or a ligand peptide for host cation-independent mannose-6-phosphate receptor[38], which will ultimately affords cross-reactivity against multiple filovirus species. Accordingly, we designed NPC2-fused AF-03 and demonstrated its broad-spectrum inhibitory capacity to filovirus species and EBOV mutants. Future investigations on the inhibition of AF03-NL to authentic virus infection in vitro and in vivo are warranted.

Overall, our study identified a high-affinity anti-MARV antibody AF-03 targeting a conserved and hidden site at the filovirus GPcl-NPC1 interface, which was capable of neutralizing MARV infection both in vitro and in vivo. Furthermore, AF-03 may be a potential candidate for the effective protection against pan-filovirus species infection. Investigations on AF-03 treatment of mice challenged by authentic virus are undergoing.

Abbreviations

MARV: Marburg virus; EBOV: Ebola virus; SUDV: Sudan virus; BDBV: Bundibugy virus; mAb: monoclonal antibody; PBS: phosphate-buffered saline; GP: glycoprotein; RAVN: Ravn virus; RESTV: Reston virus; TAFV: Tai forest virus; MVD: Marburg virus disease; EVD: EBOV virus; RBD: receptor binding domain; MLD: mucin like domain; NPC1: Niemann-Pick C1; CDR: complementarity determining region; CVFF: consistent valence force field; FV: fragment variable; CI-MPR: cation-independent mannose-6-phosphate receptor; NPC2: Niemann-Pick C2

Compliance with ethics guidelines

Yuting Zhang, Min Zhang, Haiyan Wu, Xinwei Wang, Hang Zheng, Junjuan Feng, Jing Wang, Longlong Luo, He Xiao, Chunxia Qiao, Xinying Li, Yuanqiang Zheng, Weijin Huang, Youchun Wang, Yi Wang, Yanchun Shi, Jiannan Feng, Guojiang Chen declare that they have no competing interests.

Author contributions

Guojiang Chen, Jiannan Feng, Yanchun Shi and Yi Wang conceived and designed this study. Guojiang Chen, Jiannan Feng and Yuanqiang Zheng provided funding support. Yuting Zhang, Min Zhang, Haiyan Wu and Xinwei Wang performed of the experiments and prepared the manuscript. Hang Zheng and Junjuan Feng were involved in optimization of the experimental protocols. Jing Wang, Longlong Luo, He Xiao, Chunxia Qiao, Xinying Li, Yuanqiang Zheng, Weijin Huang, Youchun Wang provided methodological support. All authors contributed to the article and approved the submitted version.

Acknowledgments

This work is granted from the National Natural Science Foundation of China (81672803, 31771010, 81871252).

Ethics approval

The animal study was reviewed and approved by the Institutional Animal Care and Use Committee of Academy of Military Medical Sciences.

References

1.Amarasinghe, G.K., Ayllón, M.A., Bào, Y., Basler, C.F., Bavari, S., Blasdell, K.R., Briese, T., Brown, P.A., Bukreyev, A., Balkema-Buschmann, A., et al. (2019). Taxonomy of the order Mononegavirales: update 2019. Arch Virol *164*, 1967-1980. 10.1007/s00705-019-04247-4.

2.Baseler, L., Chertow, D.S., Johnson, K.M., Feldmann, H., and Morens, D.M. (2017). The Pathogenesis of Ebola Virus Disease. Annu Rev Pathol *12*, 387-418. 10.1146/annurev-pathol-052016-100506.

3.Kuhn, J.H., Adachi, T., Adhikari, N.K.J., Arribas, J.R., Bah, I.E., Bausch, D.G., Bhadelia, N., Borchert, M., Brantsæter, A.B., Brett-Major, D.M., et al. (2019). New filovirus disease classification and nomenclature. Nat Rev Microbiol *17*, 261-263. 10.1038/s41579-019-0187-4.

4.Bào, Y., Amarasinghe, G.K., Basler, C.F., Bavari, S., Bukreyev, A., Chandran, K., Dolnik, O., Dye, J.M., Ebihara, H., Formenty, P., et al. (2017). Implementation of Objective PASC-Derived Taxon Demarcation Criteria for Official Classification of Filoviruses. Viruses *9*. 10.3390/v9050106.

5.Ristanović, E.S., Kokoškov, N.S., Crozier, I., Kuhn, J.H., and Gligić, A.S. (2020). A Forgotten Episode of Marburg Virus Disease: Belgrade, Yugoslavia, 1967. Microbiol Mol Biol Rev *84*. 10.1128/MMBR.00095-19.

6.Fan, P., Chi, X., Liu, G., Zhang, G., Chen, Z., Liu, Y., Fang, T., Li, J., Banadyga, L., He, S., et al. (2020). Potent neutralizing monoclonal antibodies against Ebola virus isolated from vaccinated donors. mAbs *12*, 1742457. 10.1080/19420862.2020.1742457.

7.Goldstein, T., Anthony, S.J., Gbakima, A., Bird, B.H., Bangura, J., Tremeau-Bravard, A., Belaganahalli, M.N., Wells, H.L., Dhanota, J.K., Liang, E., et al. (2018). The discovery of Bombali virus adds further support for bats as hosts of ebolaviruses. Nat Microbiol *3*, 1084-1089. 10.1038/s41564-018-0227-2.

8.Negredo, A., Palacios, G., Vázquez-Morón, S., González, F., Dopazo, H., Molero, F., Juste, J., Quetglas, J., Savji, N., de la Cruz Martínez, M., et al. (2011). Discovery of an ebolavirus-like filovirus in europe. PLoS Pathog *7*, e1002304. 10.1371/journal.ppat.1002304.

9.Kemenesi, G., Tóth, G.E., Mayora-Neto, M., Scott, S., Temperton, N., Wright, E., Mühlberger, E., Hume, A.J., Suder, E.L., Zana, B., et al. (2022). Isolation of infectious Lloviu virus from Schreiber's bats in Hungary. Nat Commun *13*, 1706. 10.1038/s41467-022-29298-1.

10.Yang, X.L., Tan, C.W., Anderson, D.E., Jiang, R.D., Li, B., Zhang, W., Zhu, Y., Lim, X.F., Zhou, P., Liu, X.L., et al. (2019). Characterization of a filovirus (Měnglà virus) from Rousettus bats in China. Nat Microbiol *4*, 390-395. 10.1038/s41564-018-0328-y.

11.Mehedi, M., Groseth, A., Feldmann, H., and Ebihara, H. (2011). Clinical aspects of Marburg hemorrhagic fever. Future Virol *6*, 1091-1106. 10.2217/fvl.11.79.

12.Beniac, D.R., and Booth, T.F. (2017). Structure of the Ebola virus glycoprotein spike within the virion envelope at 11 A resolution. Sci Rep *7*, 46374. 10.1038/srep46374.

13.Lee, J.E., and Saphire, E.O. (2009). Neutralizing ebolavirus: structural insights into the envelope glycoprotein and antibodies targeted against it. Curr Opin Struct Biol *19*, 408-417. 10.1016/j.sbi.2009.05.004.

14.Brauburger, K., Hume, A.J., Mühlberger, E., and Olejnik, J. (2012). Forty-five years of Marburg virus research. Viruses *4*, 1878-1927. 10.3390/v4101878.

15.Schafer, A., Xiong, R., Cooper, L., Nowar, R., Lee, H., Li, Y., Ramirez, B.E., Peet, N.P., Caffrey, M., Thatcher, G.R.J., et al. (2021). Evidence for distinct mechanisms of small molecule inhibitors of filovirus entry. PLoS Pathog *17*, e1009312. 10.1371/journal.ppat.1009312.

16.Hashiguchi, T., Fusco, M.L., Bornholdt, Z.A., Lee, J.E., Flyak, A.I., Matsuoka, R., Kohda, D., Yanagi, Y.,

508 Hammel, M., Jr, J.E.C., and Saphire, E.O. (2015). Structural basis for Marburg virus neutralization by a
509 cross-reactive human antibody. Cell *160*, 904-912. 10.1016/j.cell.2015.01.041.
510 17.Fusco, M.L., Hashiguchi, T., Cassan, R., Biggins, J.E., Murin, C.D., Warfield, K.L., Li, S., Holtsberg, F.W.,
511 Shulenin, S., Vu, H., et al. (2015). Protective mAbs and Cross-Reactive mAbs Raised by Immunization
512 with Engineered Marburg Virus GPs. PLoS Pathog *11*, e1005016. 10.1371/journal.ppat.1005016.
513 18.Gregory, S.M., Harada, E., Liang, B., Delos, S.E., White, J.M., and Tamm, L.K. (2011). Structure and
514 function of the complete internal fusion loop from Ebolavirus glycoprotein 2. Proc Natl Acad Sci U S A
515 *108*, 11211-11216. 10.1073/pnas.1104760108.
516 19.Lee, J., Nyenhuis, D.A., Nelson, E.A., Cafiso, D.S., White, J.M., and Tamm, L.K. (2017). Structure of
517 the Ebola virus envelope protein MPER/TM domain and its interaction with the fusion loop explains
518 their fusion activity. Proc Natl Acad Sci U S A *114*, E7987-E7996. 10.1073/pnas.1708052114.
519 20.Volchkov, V.E., Volchkova, V.A., Ströher, U., Becker, S., Dolnik, O., Cieplik, M., Garten, W., Klenk, H.D.,
520 and Feldmann, H. (2000). Proteolytic processing of Marburg virus glycoprotein. Virology *268*, 1-6.
521 10.1006/viro.1999.0110.
522 21.Dye, J.M., Herbert, A.S., Kuehne, A.I., Barth, J.F., Muhammad, M.A., Zak, S.E., Ortiz, R.A., Prugar, L.I.,
523 and Pratt, W.D. (2012). Postexposure antibody prophylaxis protects nonhuman primates from filovirus
524 disease. Proc Natl Acad Sci U S A *109*, 5034-5039. 10.1073/pnas.1200409109.
525 22.Aleksandrowicz, P., Marzi, A., Biedenkopf, N., Beimforde, N., Becker, S., Hoenen, T., Feldmann, H.,
526 and Schnittler, H.-J. (2011). Ebola virus enters host cells by macropinocytosis and clathrin-mediated
527 endocytosis. J Infect Dis *204 Suppl 3*, S957-967. 10.1093/infdis/jir326.
528 23.Saeed, M.F., Kolokoltsov, A.A., Albrecht, T., and Davey, R.A. (2010). Cellular entry of ebola virus
529 involves uptake by a macropinocytosis-like mechanism and subsequent trafficking through early and
530 late endosomes. PLoS Pathog *6*, e1001110. 10.1371/journal.ppat.1001110.
531 24.Carette, J.E., Raaben, M., Wong, A.C., Herbert, A.S., Obernosterer, G., Mulherkar, N., Kuehne, A.I.,
532 Kranzusch, P.J., Griffin, A.M., Ruthel, G., et al. (2011). Ebola virus entry requires the cholesterol
533 transporter Niemann-Pick C1. Nature *477*, 340-343. 10.1038/nature10348.
534 25.Brecher, M., Schornberg, K.L., Delos, S.E., Fusco, M.L., Saphire, E.O., and White, J.M. (2012).
535 Cathepsin cleavage potentiates the Ebola virus glycoprotein to undergo a subsequent fusion-relevant
536 conformational change. J Virol *86*, 364-372. 10.1128/JVI.05708-11.
537 26.Martinez, O., Johnson, J., Manicassamy, B., Rong, L., Olinger, G.G., Hensley, L.E., and Basler, C.F.
538 (2010). Zaire Ebola virus entry into human dendritic cells is insensitive to cathepsin L inhibition.
539 Cellular Microbiology *12*, 148-157. 10.1111/j.1462-5822.2009.01385.x.
540 27.Gnirss, K., Kühl, A., Karsten, C., Glowacka, I., Bertram, S., Kaup, F., Hofmann, H., and Pöhlmann, S.
541 (2012). Cathepsins B and L activate Ebola but not Marburg virus glycoproteins for efficient entry into
542 cell lines and macrophages independent of TMPRSS2 expression. Virology *424*, 3-10.
543 10.1016/j.virol.2011.11.031.
544 28.Misasi, J., Chandran, K., Yang, J.-Y., Considine, B., Filone, C.M., Côté, M., Sullivan, N., Fabozzi, G.,
545 Hensley, L., and Cunningham, J. (2012). Filoviruses require endosomal cysteine proteases for entry but
546 exhibit distinct protease preferences. J Virol *86*, 3284-3292. 10.1128/JVI.06346-11.
547 29.Hu, N., Qiao, C., Wang, J., Wang, Z., Li, X., Zhou, L., Wu, J., Zhang, D., Feng, J., Shen, B., et al. (2021).
548 Identification of a novel protective human monoclonal antibody, LXY8, that targets the key
549 neutralizing epitopes of staphylococcal enterotoxin B. Biochem Biophys Res Commun *549*, 120-127.
550 10.1016/j.bbrc.2021.02.057.
551 30.Wang, Z., Hu, N., Zhou, Y., Shi, N., Shen, B., Luo, L., and Feng, J. (2022). Structure-guided affinity

552 maturation of a novel human antibody targeting the SARS-CoV-2 nucleocapsid protein. Scientific
553 Reports *12*, 8469. 10.1038/s41598-022-12242-0.
554 31.Dahms, N.M., Olson, L.J., and Kim, J.J. (2008). Strategies for carbohydrate recognition by the
555 mannose 6-phosphate receptors. Glycobiology *18*, 664-678. 10.1093/glycob/cwn061.
556 32.Bohnsack, R.N., Song, X., Olson, L.J., Kudo, M., Gotschall, R.R., Canfield, W.M., Cummings, R.D.,
557 Smith, D.F., and Dahms, N.M. (2009). Cation-independent mannose 6-phosphate receptor: a
558 composite of distinct phosphomannosyl binding sites. J Biol Chem *284*, 35215-35226.
559 10.1074/jbc.M109.056184.
560 33.Grubb, J.H., Vogler, C., and Sly, W.S. (2010). New strategies for enzyme replacement therapy for
561 lysosomal storage diseases. Rejuvenation Res *13*, 229-236. 10.1089/rej.2009.0920.
562 34.Duan, Y., Luo, L., Qiao, C., Li, X., Wang, J., Liu, H., Zhou, T., Shen, B., Lv, M., and Feng, J. (2019). A
563 novel human anti-AXL monoclonal antibody attenuates tumour cell migration. Scandinavian journal of
564 immunology. 10.1111/sji.1277.
565 35.Liu, F., Guan, Z., Liu, Y., Li, J., Liu, C., Gao, Y., Ma, Y., Feng, J., Shen, B., and Yang, G. (2021).
566 Identification of a Human Anti-Alpha-Toxin Monoclonal Antibody Against Staphylococcus aureus
567 Infection. Frontiers in Microbiology *12*, 1875-. 10.3389/fmicb.2021.692279.
568 36.Markosyan, R.M., Miao, C., Zheng, Y.-M., Melikyan, G.B., Liu, S.-L., and Cohen, F.S. (2016). Induction
569 of Cell-Cell Fusion by Ebola Virus Glycoprotein: Low pH Is Not a Trigger. PLoS Pathog *12*, e1005373.
570 10.1371/journal.ppat.1005373.
571 37.Shifflett, K., and Marzi, A. (2019). Marburg virus pathogenesis - differences and similarities in
572 humans and animal models. Virol J *16*, 165. 10.1186/s12985-019-1272-z.
573 38.Wirchnianski, A.S., Wec, A.Z., Nyakatura, E.K., Herbert, A.S., Slough, M.M., Kuehne, A.I., Mittler, E.,
574 Jangra, R.K., Teruya, J., Dye, J.M., et al. (2021). Two Distinct Lysosomal Targeting Strategies Afford
575 Trojan Horse Antibodies With Pan-Filovirus Activity. Frontiers in immunology *12*, 729851.
576 10.3389/fimmu.2021.729851.
577 39.Abir, M.H., Rahman, T., Das, A., Etu, S.N., Nafiz, I.H., Rakib, A., Mitra, S., Emran, T.B., Dhama, K.,
578 Islam, A., et al. (2022). Pathogenicity and virulence of Marburg virus. Virulence *13*, 609-633.
579 10.1080/21505594.2022.2054760.
580 40.Araf, Y., Maliha, S.T., Zhai, J., and Zheng, C. (2023). Marburg virus outbreak in 2022: a public health
581 concern. Lancet Microbe *4*, e9. 10.1016/s2666-5247(22)00258-0.
582 41.Flyak, A.I., Ilinykh, P.A., Murin, C.D., Garron, T., Shen, X., Fusco, M.L., Hashiguchi, T., Bornholdt, Z.A.,
583 Slaughter, J.C., Sapparapu, G., et al. (2015). Mechanism of human antibody-mediated neutralization of
584 Marburg virus. Cell *160*, 893-903. 10.1016/j.cell.2015.01.031.
585 42.Marzi, A., Haddock, E., Kajihara, M., Feldmann, H., and Takada, A. (2018). Monoclonal Antibody
586 Cocktail Protects Hamsters From Lethal Marburg Virus Infection. J Infect Dis *218*, S662-S665.
587 10.1093/infdis/jiy235.
588 43.Kan, S.H., Troitskaya, L.A., Sinow, C.S., Haitz, K., Todd, A.K., Di Stefano, A., Le, S.Q., Dickson, P.I., and
589 Tippin, B.L. (2014). Insulin-like growth factor II peptide fusion enables uptake and lysosomal delivery
590 of α-N-acetylglucosaminidase to mucopolysaccharidosis type IIIB fibroblasts. Biochem J *458*, 281-289.
591 10.1042/bj20130845.
592 44.Aoyagi-Scharber, M., Crippen-Harmon, D., Lawrence, R., Vincelette, J., Yogalingam, G., Prill, H., Yip,
593 B.K., Baridon, B., Vitelli, C., Lee, A., et al. (2017). Clearance of Heparan Sulfate and Attenuation of CNS
594 Pathology by Intracerebroventricular BMN 250 in Sanfilippo Type B Mice. Mol Ther Methods Clin Dev

595 *6*, 43-53. 10.1016/j.omtm.2017.05.009.
596 45.Kan, S.H., Aoyagi-Scharber, M., Le, S.Q., Vincelette, J., Ohmi, K., Bullens, S., Wendt, D.J.,
597 Christianson, T.M., Tiger, P.M., Brown, J.R., et al. (2014). Delivery of an enzyme-IGFII fusion protein to
598 the mouse brain is therapeutic for mucopolysaccharidosis type IIIB. Proc Natl Acad Sci U S A *111*,
599 14870-14875. 10.1073/pnas.1416660111.
600 46.Berthe, M.L., Esslimani Sahla, M., Roger, P., Gleizes, M., Lemamy, G.J., Brouillet, J.P., and Rochefort,
601 H. (2003). Mannose-6-phosphate/insulin-like growth factor-II receptor expression levels during the
602 progression from normal human mammary tissue to invasive breast carcinomas. Eur J Cancer *39*,
603 635-642. 10.1016/s0959-8049(02)00627-5.
604 47.Jonson, T., Albrechtsson, E., Axelson, J., Heidenblad, M., Gorunova, L., Johansson, B., and Höglund,
605 M. (2001). Altered expression of TGFB receptors and mitogenic effects of TGFB in pancreatic
606 carcinomas. Int J Oncol *19*, 71-81.
607 48.Pavelić, K., Kolak, T., Kapitanović, S., Radosević, S., Spaventi, S., Kruslin, B., and Pavelić, J. (2003).
608 Gastric cancer: the role of insulin-like growth factor 2 (IGF 2) and its receptors (IGF 1R and M6-P/IGF
609 2R). J Pathol *201*, 430-438. 10.1002/path.1465.
610 49.Densumite, J., Phanthong, S., Seesuay, W., Sookrung, N., Chaisri, U., and Chaicumpa, W. (2021).
611 Engineered Human Monoclonal scFv to Receptor Binding Domain of Ebolavirus. Vaccines *9*.
612 10.3390/vaccines9050457.

613

614

Figure legends

Figure 1. Binding activity of mAb AF-03 to MARV GP and its epitopes.

(A) AF-03 and MARV GP proteins are examined by SDS-PAGE. NR, non-reducing; R, reducing. (B) The binding activity of AF-03 to MARV GP is determined by ELISA. The absorbance is detected at 450 nm. (C) The binding kinetics of AF-03 to MARV GP is detected by BLI with a 180-s association step followed by a 220-s dissociation step. Experiments are independently repeated at least three times, and the data from one representative experiment is shown. (D) The 3-D ribbon structures of the AF-03 Fv fragment. The red ribbon denotes H-CDR1, the light blue denotes H-CDR2, the pink denotes H-CDR3, the orange denotes L-CDR1, the deep blue denotes L-CDR2, the purple denotes L-CDR3. (E) AF-03 and MARV GP complex derived from theoretical modeling. The green ribbon denotes the orientation of the MARV GP fragment, the yellow denotes AF-03 VLCDR, the pink denotes AF-03 VHCDR, the deep blue denotes AF-03 VL and the red ribbon denotes AF-03 VH. (F) By molecular docking analysis of van der Waals interaction, intermolecular hydrogen bonding, polarity interaction and electrostatic interaction, the key amino acid residues of MARV GP are screened.

Figure 2. AF-03 Epitope Identification.

(A) The neutralization activity of AF-03 or MR78 to mutated pseudovirus ($Q^{128}S$-$N^{129}S$, $Q^{204}A$-$T^{205}A$-$Q^{206}A$, $Y^{218}A$, $K^{222}A$, $C^{226}Y$) is evaluated in HEK293T cells. The inhibition rate is analyzed. (B) The binding of AF-03 and MR78 to mutant

GP ($Q^{128}S$-$N^{129}S$ or $C^{226}Y$) is examined by ELISA respectively. (C) Secondary structure of mutants and MARV GP is detected by CD. (D) The epitope overlapping between AF-03 and MR78 is examined by the competition ELISA.

Figure 3. In vitro and in vivo neutralization of MARV pseudovirus infection by AF-03.

(A) Pseudotypic MARV-Uganda is incubated with AF-03, MR78 or control mAb at 37°C for 1 h before infecting HEK293T cells (left) and Huh7 cells (right) respectively. Luciferase is assayed and inhibition rates are calculated. (B) Pseudotypic MARV-Angola, Musoke and Ravn infect HEK293T cells respectively and neutralization activity of AF-03 to these species is determined. (C) AF-03 (10, 3, 1mg/kg) is administrated at 24 and 4 h before intraperitoneal injection of pseudovirus. On day 5, bioluminescence signals are detected by an IVIS Lumina Series III imaging system. (D) The average radiance value based on the luminescence of (C),*$*p<0.05$, $**p<0.01$, $***p<0.001$.*

Figure 4. The neutralization activity of AF-03 to EBOV, SUDV and BDBV harboring cleaved GP.

Pseudotypic EBOV, SUDV, and BDBV are processed with thermolysin at 37°C. Inhibition of these ebola virus infection harboring GP or GPcl by AF-03 is examined by luciferase assay. *$*p<0.05$, $**p<0.01$, $***p<0.001$*

Figure 5. Cellular internalization of AF03-NL.

(A) AF-03 or AF03-NL is incubated with cells at 4□ for 1h to prevent internalization and then at 37□ for another 2 h to allow internalization. PE-conjugated secondary antibody is added prior to analysis by flow cytometry. (B,C) pHrodo Red-labelled AF-03 or AF03-NL is incubated with cells at 37□ for 1h and analyzed by flow cytometry (B) and fluorescence microscopy (C) respectively. The red arrow denotes internalized AF03-NL. Experiments are independently repeated at least three times, and the data from one representative experiment is shown.

Figure 6. Pan-filovirus entry inhibition by AF03-NL.

(A,B) AF-03 or AF03-NL is incubated with HEK293T cells at 37°C for 2 h prior to exposure to pseudotypic filovirus species (A) and EBOV mutants (B). Luciferase is assayed and inhibition rates are calculated.

Figure 7. The requirement of CI-MPR for the neutralization activity of AF03-NL.

(A) NPC2 protein is examined by SDS-PAGE. NR, non-reducing; R, reducing. (B) AF03-NL, AF-03, NPC2 alone or equimolar combination of AF-03 and NPC2 is incubated with HEK293T cells at 37°C for 2 h prior to exposure to pseudotypic EBOV. Luciferase is assayed and inhibition rates are calculated. (C) HEK293T cells are treated with siRNA-CI-MPR or negative control vector (NC) respectively and CI-MPR expression is detected by flow cytometry. AF03-NL is incubated with

siCI-MPR or NC-treated HEK293T cells at 37°C for 2 h respectively prior to exposure to pseudotypic EBOV. (D) CI-MPR is introduced into Huh7 cells and its expression is detected by flow cytometry. AF03-NL is incubated with CI-MPR or NC-knockin Huh7 cells at 37°C for 2 h respectively prior to exposure to pseudotypic EBOV. Luciferase is assayed and inhibition rates are calculated.

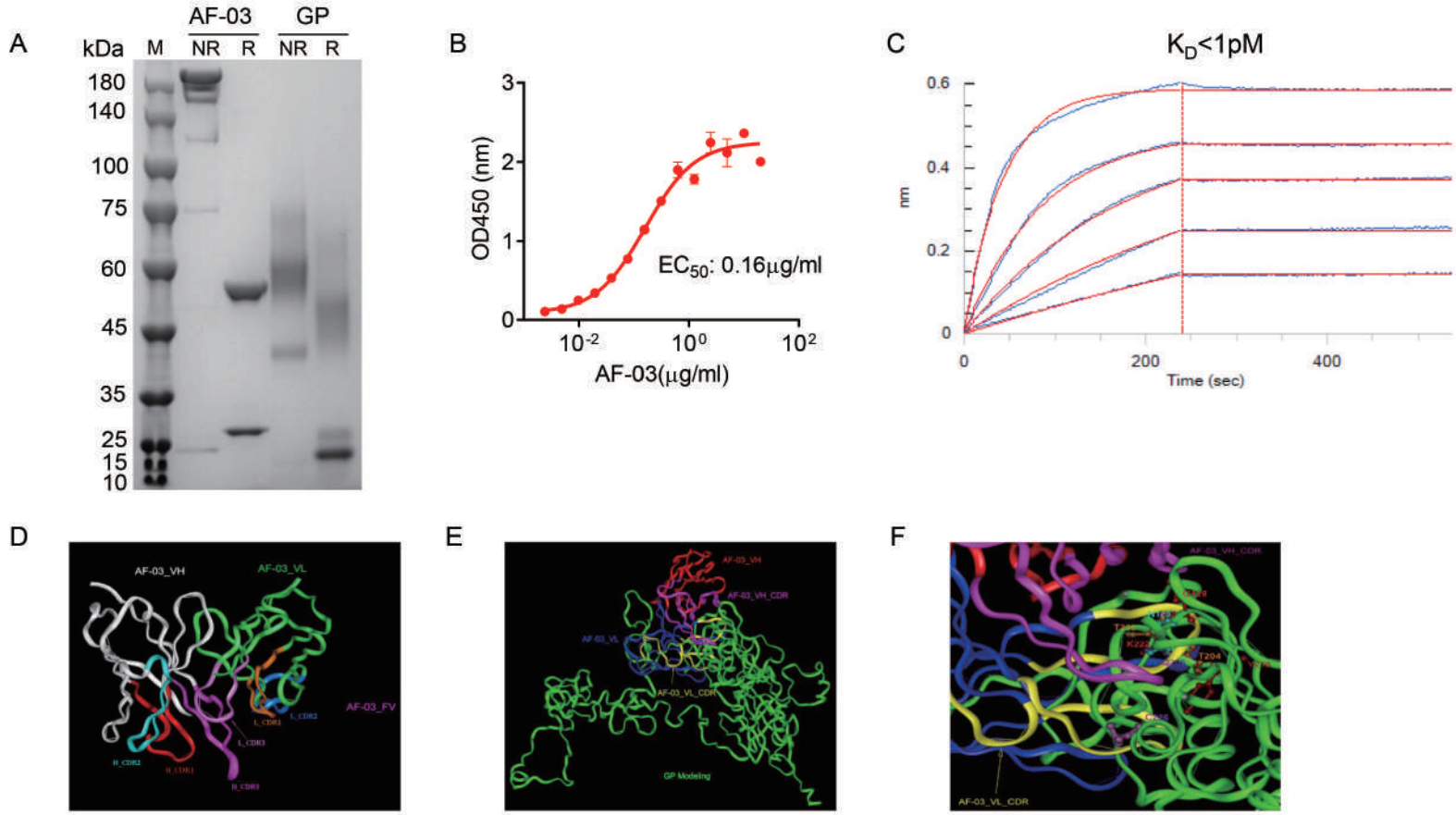
A
kDa
M
AF-03
GP
NR
R
NR
R
180
140
100
75
60
45
35
25
15
10
B
OD450 (nm)
EC50: 0.16μg/ml
AF-03(μg/ml)
C
KD<1pM
nm
Time (sec)
D
AF-03_VH
AF-03_VL
AF-03_FV
E
F
AF-03_VL_CDR

A

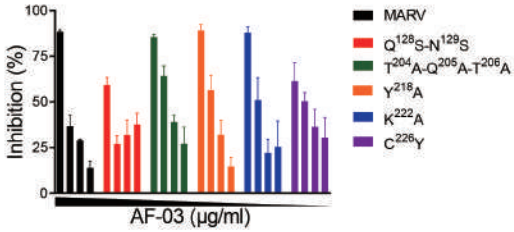
Inhibition (%)
100
75
50
25
0
AF-03 (μg/ml)
MARV
Q128S-N129S
T204A-Q205A-T206A
Y218A
K222A
C226Y

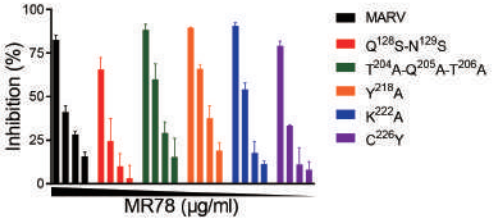
Inhibition (%)
100
75
50
25
0
MR78 (μg/ml)
MARV
Q128S-N129S
T204A-Q205A-T206A
Y218A
K222A
C226Y

B

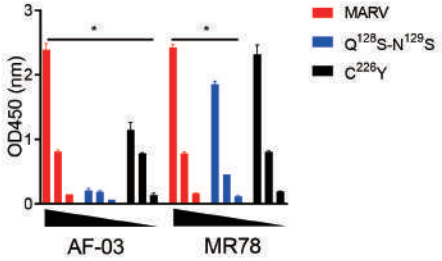
OD450 (nm)
3
2
1
0
*
*
AF-03
MR78
MARV
Q128S-N129S
C226Y

C

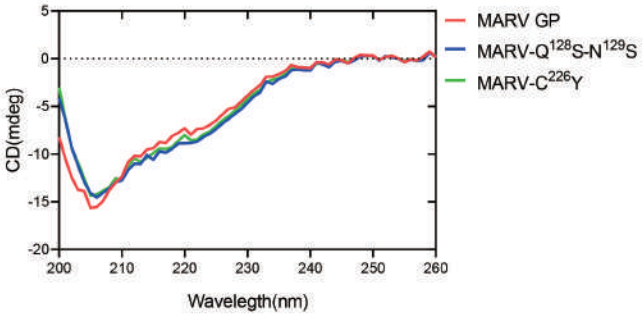
CD(mdeg)
5
0
-5
-10
-15
-20
200
210
220
230
240
250
260
Wavelegth(nm)
MARV GP
MARV-Q128S-N129S
MARV-C226Y

D

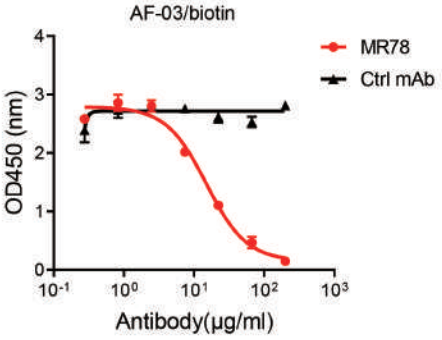
AF-03/biotin
OD450 (nm)
4
3
2
1
0
10-1
100
101
102
103
Antibody(μg/ml)
MR78
Ctrl mAb

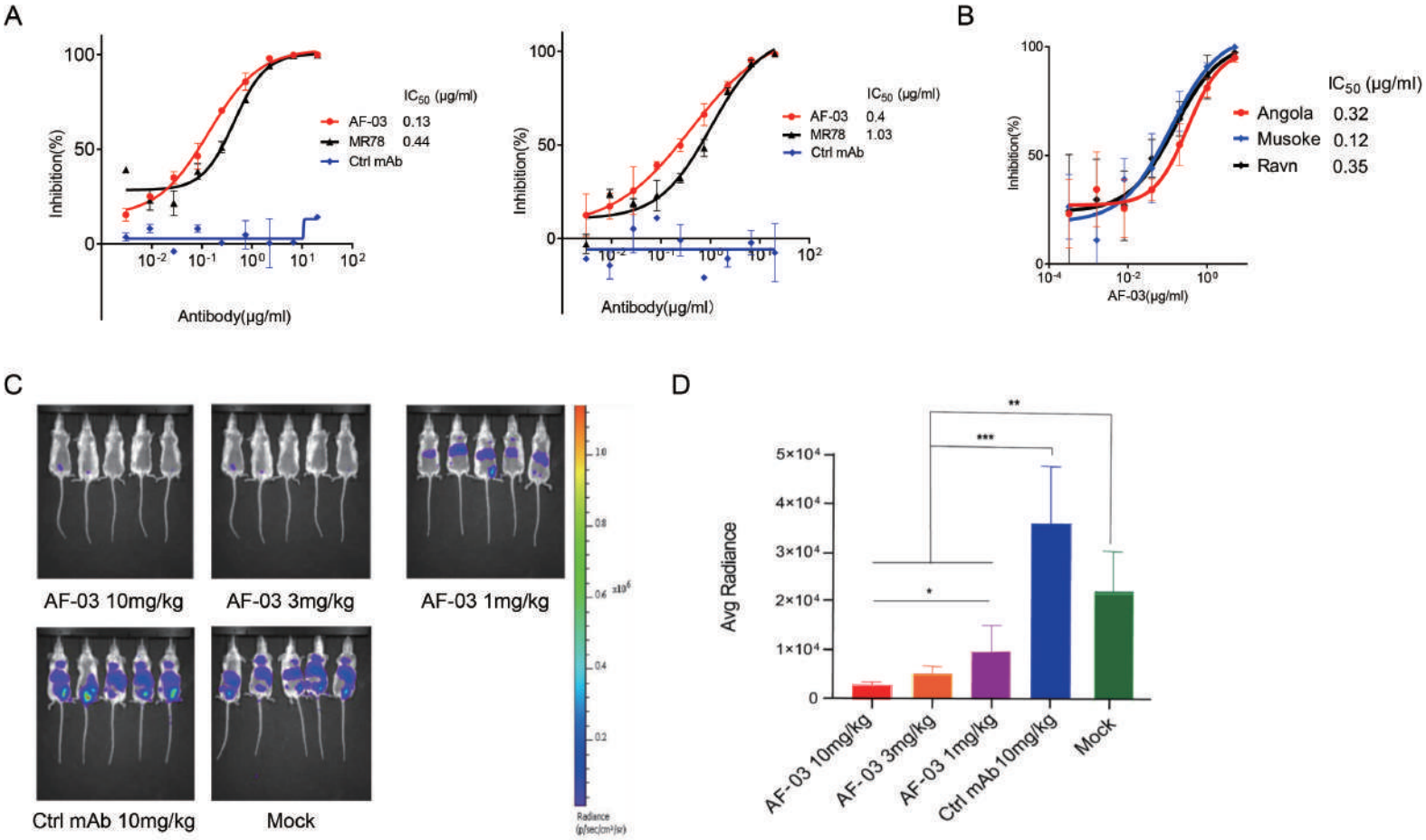
A
Inhibition(%)
Antibody(μg/ml)
IC50 (μg/ml)
AF-03 0.13
MR78 0.44
Ctrl mAb
AF-03 0.4
MR78 1.03
B
Angola 0.32
Musoke 0.12
Ravn 0.35
AF-03(μg/ml)
C
AF-03 10mg/kg
AF-03 3mg/kg
AF-03 1mg/kg
Ctrl mAb 10mg/kg
Mock
D
Avg Radiance
AF-03 10mg/kg
AF-03 3mg/kg
AF-03 1mg/kg
Ctrl mAb 10mg/kg
Mock

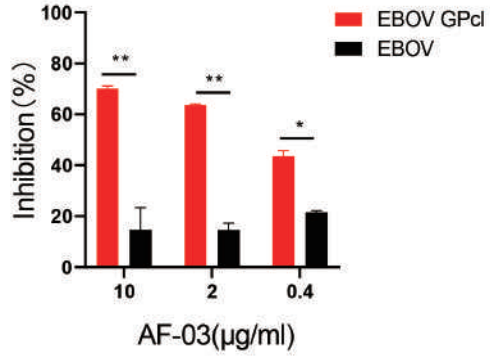
EBOV GPcl
EBOV
Inhibition (%)
100
80
60
40
20
0
**
**
*
10
2
0.4
AF-03(μg/ml)

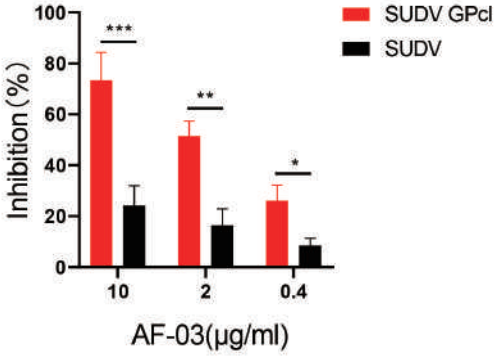
SUDV GPcl
SUDV
Inhibition (%)
100
80
60
40
20
0
***
**
*
10
2
0.4
AF-03(μg/ml)

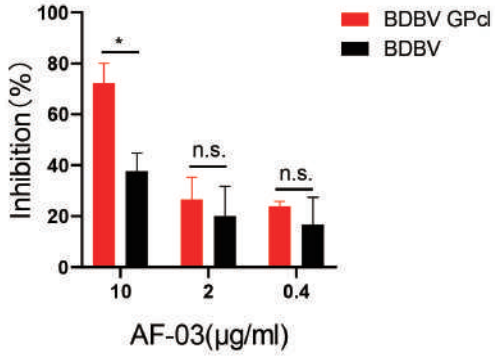
BDBV GPcl
BDBV
Inhibition (%)
100
80
60
40
20
0
*
n.s.
n.s.
10
2
0.4
AF-03(μg/ml)

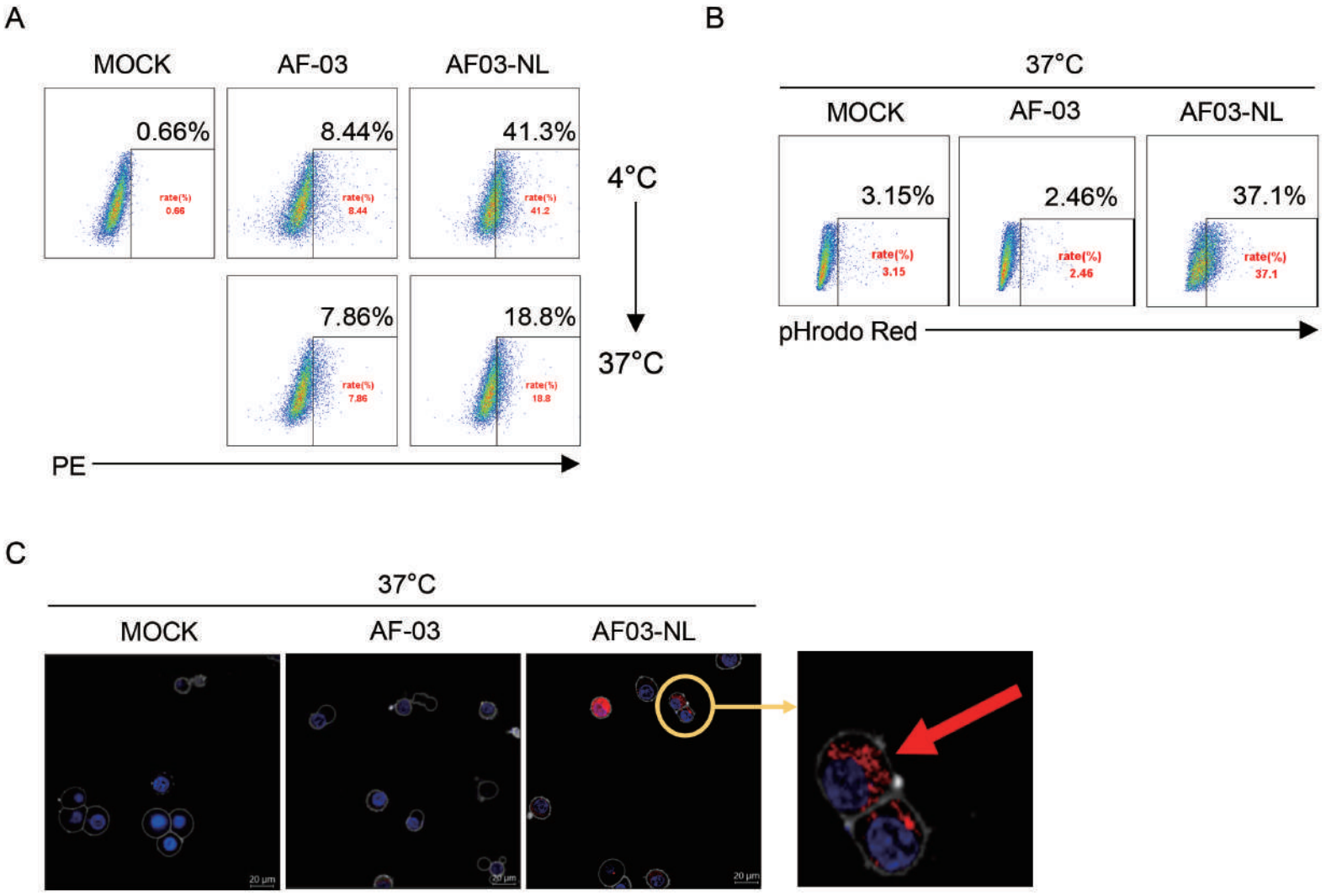
A
MOCK
AF-03
AF03-NL
0.66%
8.44%
41.3%
4°C
7.86%
18.8%
37°C
PE
B
37°C
MOCK
AF-03
AF03-NL
3.15%
2.46%
37.1%
pHrodo Red
C
37°C
MOCK
AF-03
AF03-NL
20 μm

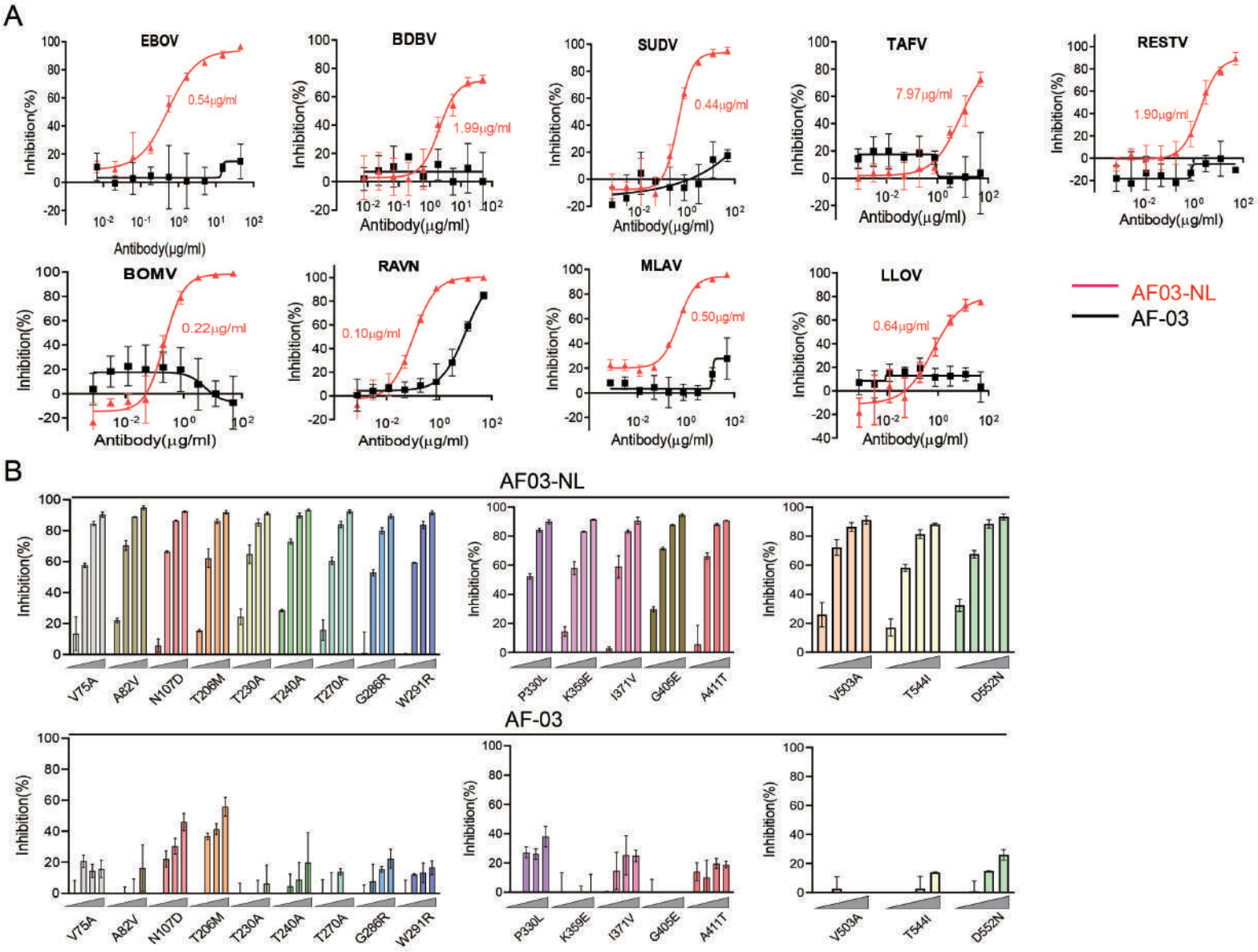
A
EBOV
0.54μg/ml
BDBV
1.99μg/ml
SUDV
0.44μg/ml
TAFV
7.97μg/ml
RESTV
1.90μg/ml
BOMV
0.22μg/ml
RAVN
0.10μg/ml
MLAV
0.50μg/ml
LLOV
0.64μg/ml
Inhibition(%)
Antibody(μg/ml)
AF03-NL
AF-03
B
AF03-NL
AF-03
V75A
A82V
N107D
T206M
T230A
T240A
T270A
G286R
W291R
P330L
K359E
I371V
G405E
A411T
V503A
T544I
D552N

A

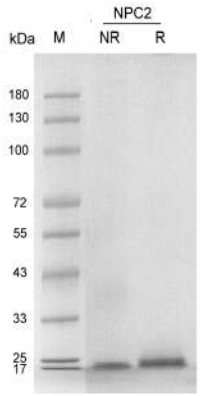
NPC2
kDa
M
NR
R
180
130
100
72
55
43
33
25
17

B

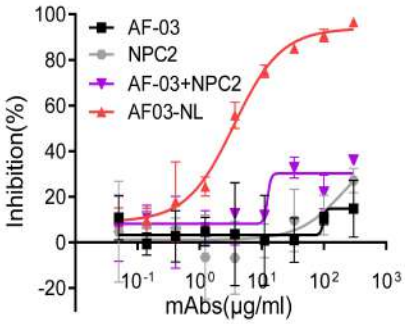
AF-03
NPC2
AF-03+NPC2
AF03-NL
Inhibition(%)
mAbs(μg/ml)

C

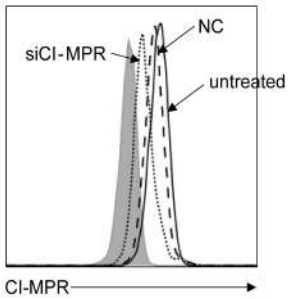
siCI-MPR
NC
untreated
CI-MPR

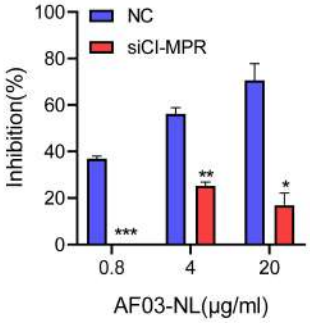
NC
siCI-MPR
Inhibition(%)
AF03-NL(μg/ml)

D

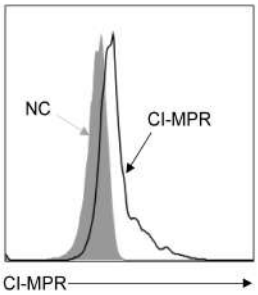
NC
CI-MPR
CI-MPR

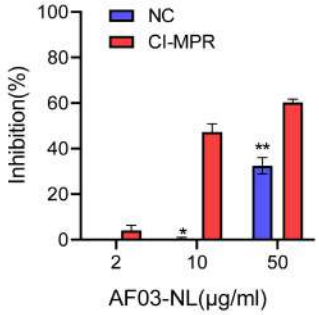
NC
CI-MPR
Inhibition(%)
AF03-NL(μg/ml)